Development of Cost-Effective Automated Test System for Determining Lifetime of Gold Contacts Under Mechanical Load

H. Alaboz[1], A. Kovacs[1], Y. Safa[2], and U. Mescheder[1,3]
[1]Institute for Microsystems Technology (IMST), Furtwangen University, 78120 Furtwangen, Germany
[2]Zürcher Hochschule für Angewandte Wissenschaften (ZHAW), 8400 Winterthur, Switzerland
[3]Associated to the Faculty of Engineering, University of Freiburg, 79110 Freiburg im Breisgau, Germany
e-mail: alz@hs-furtwangen.de

Abstract

Mechanic load tests for electrical contacts for different components have been performed and related standards have been developed for various use cases. Even though there are readily available literature and standards, conditions of the testing for various components under mechanical loading remain similar. Real life operating conditions usually different then the testing conditions and even the slight differences can influence the precision of the prediction mechanisms. We propose an automated mechanical loading system to mimic real life operating condition and test lifetime of the contact parts. A cost effective, compact experimental test system was designed, produced and tested for stability issues. The automated test system successfully completed one million mechanical loading cycles on the samples and surface deformations as well as lifetime of some contact components were determined. A correlation has been found between computational model and the experimental results.

1 Introduction

Lifetime and failure prediction of contacts in various fields have been investigated due to their importance in crucial components such as mechanical relays [1] and solar panels [2]. Due to continuously rising demand of metals in crucial industrial sectors, demand for low prices and scarcity of metal resources create demand for better predictive testing, standards and systems. Failure mechanism and surface deformations on metal contact surfaces heavily depend on the type and the condition of the loading mechanism [1-5]. In this study, we concentrated on the lifetime of a metal contact comb-rubber dome structure under automated and repetitive mechanical load. Even though existing automated industrial test machines are fast and reliable, they are not designed to test specific cases and can be improved to mimic real operation conditions more efficiently. They are also not widely available for mid-sized companies. Therefore, a cost effective, compact and efficient automated test systems that can mimic real-life conditions better are always in demand.

2 Computational Modelling

Computational modeling at ICP ZHAW makes a complementary with automated experimental tests established at HFU for a perspective of a model-based button's design. Indeed, numerical simulations were conducted using input from experimental setup, like surface roughness, loading rate and force inclination. In the first step, modeling was based on a global approach by solving an elasto-dynamic friction contact problem on the whole contact surface using an open-source finite element package [6] **(Figure 1).** This calculation was conducted under following input conditions:

- Strip vertical motion at 10 cm/s
- Foundation horizontal motion at 20 cm/s
- Friction coefficient $\mu = 0.1$
- Yield stress $\sigma_Y = 50$ MPa
- 2D Strip gold domain of 40 µm length

A local contact area of high shear-stress was identified.

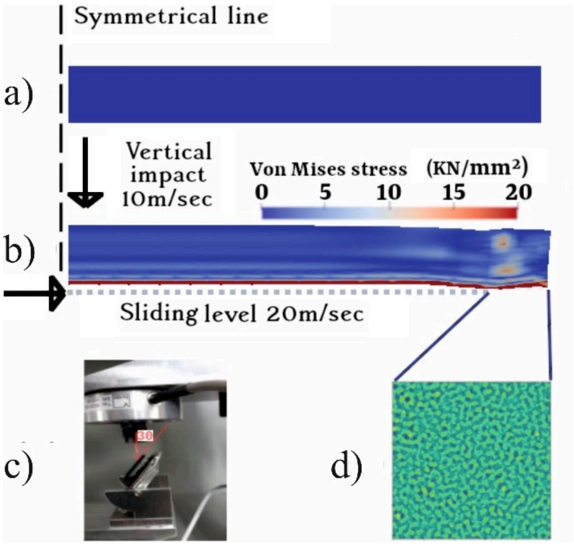

Figure 1 Global FEM approach of dynamic sliding friction contact: a) Strip simulation in vertical motion of 10 m/sec before impact. (b) Strip is reaching the foundation level undergoing a sliding speed of 20 m/sec, the deformations are scaled for visualization and Von Mises stress are shown dominant on the side part. c) experimental setup with inclined loading test. (d) A patch sub-domain is identified of concentrated stress region to be analysed using local adhesive wear model.

In second step, a local approach was applied using boundary integral method to solve adhesive contact problem **(Figure 2)** in aforementioned local area. A random-height rough surface was generated corresponding to measured surface amplitudes **Figure 1 (d)**.

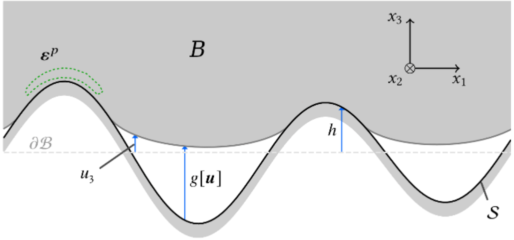

Figure 2 Schematic representation of a periodic elastic-plastic contact problem, B: Elastic-plastic body is represented in deformed shape, where h is the height and u is the displacement.

This local modelling approach is based on solving a mathematical system of contact problem that is summarized as follows: A function gap between two surfaces is depending on the displacement field and the surface height:

$$g[u] = ue_3|_{\partial B} - h$$

The model is constrained by the following Hertz-Signorini-Moreau conditions:

$$g[u] \geq 0,$$
$$p[u] = T[u]e_3 \geq 0,$$
$$g[u]p[u] = 0$$

Considering the strain tensor defined linearly as:

$$\epsilon[u] = \frac{1}{2}(\nabla u + \nabla u^T)$$

the Cauchy stress tensor is given by:

$$\sigma[u, \epsilon^p] = C: (\epsilon[u] - \epsilon^p)$$

where C is the elastic tensor and ϵ^p is the plastic strain. The static force equilibrium is given by

$$\nabla . \sigma = 0 \quad \text{in plastic body B}$$

The traction force along the outer normal vector n of the boundary of the domain is given by:

$$T[u, \epsilon^p] = \sigma[u, \epsilon^p]_{\partial B} n$$

One can split the displacement field u into elastic and plastic components:

$$u = v + N[C: \epsilon^p]$$

The boundary integral method is based on the energy minimizing of the potential energy of the system. It is to find u verifying:

$$inf \left\{ \frac{1}{2} \int_{\partial B} T\,[v] v dS \right\}$$

such that (no-penetration constraint):

$$g\left[v + N[C: \epsilon^p]\right] \geq 0$$

The adhesive effect is incorporated in the contact model by considering the total potential energy as summation of elastoplastic energy and adhesive energy:

$$E_{potential} = E_{elasticplastic} + E_{adhesion}$$

where the adhesion energy is defined as

$$E_{adhesion} = -\gamma \int_S exp\left(\frac{-g}{\rho}\right) dS$$

Here γ is the surface energy and ρ is the adhesive characteristic length and *g* is gap function (**Figure 2).** Local contact problem was solved in the Fourier domain of the generated surface spectrum allowing a computational time which is two-order of magnitude faster than traditional FEM [7]. Traction, contact and adhesive zones were obtained in the local contact surface (**Figure 3).**

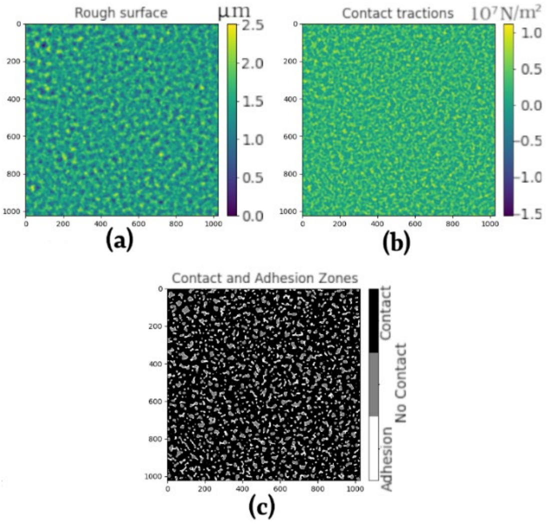

Figure 3 (a) Generated local rough surface. (b) Space distribution of adhesive contact forces. (c) Distribution of contact and adhesion zones.

3 Design of the Automated Test System

Commercial automated loading systems usually apply mechanical load normal to the sample surface. In this study the automated system was designed to mimic a specific real-life condition and test the electrical contact components durability under inclined mechanical loading. 2 phases Nema 17 stepper motor with step angle of 1.8° was used for movement and the stepper motor was controlled by Arduino. Burster 8523 compression sensor with a measurement range between 0-100 N and a deviation of 0.1 % was used as a sensor. Sensor and specifically designed sample holder were placed on V rails, pulley-belt-gantry plate system was used for smooth movement. Four-tips were designed to test four samples at once and alignment was made between tips and samples. Alignment and the design of the system was shown in **Figure 4** below.

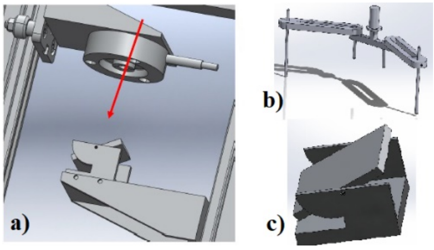

Figure 4 a) Designed system with sensor head and sample holder (red arrow represents alignment between sensor and sample holder) b) Four tips for multiple tests samples. c) Designed sample holder (inclination can be arranged according to need).

The designed system was modified and upgraded over time and some tests such as vibration, temperature and movement nonlinearity were performed to ensure the stability of the system. Automated system can apply 2.5-3 N for each cycle and the duration of the loading cycle (load and unload) is as short as four second. Duration of one cycle was reduced to one second with a slightly higher deviation value of applied force. Applied forces and number of cycles can be monitored instantaneously via Digivision data acquisition system and Arduino. As an example, a small portion of acquired data is shown in **Figure 5**.

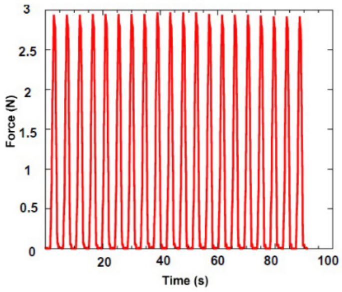

Figure 5 Measured applied force over 90 seconds. Precision and stability of the applied load can be seen from the graph.

4 Experimental Results

Electrical contact mechanism consists of two surfaces made of two different materials. One of the surfaces is an electrically conductive plastic dome and the other surface is a gold comb as shown in **Figure 6**. Lifetime of both surfaces were investigated through one million repetitive load (2.5-3 N) cycles. Optical images of the gold comb were acquired by Zeiss Axiovision optical microscope and analysed by Mountains SPIP software.

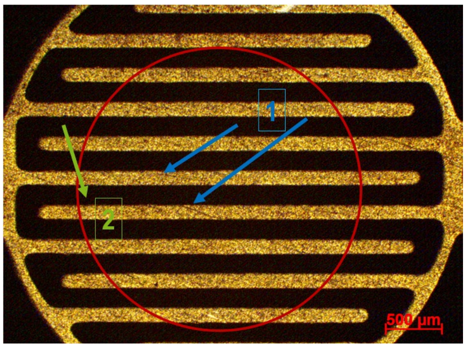

Figure 6 Optical image of the gold comb under test. Regions 1 and 2 show typical surface defects after one million load cycles. Red circle represents the full contact area.

Typically observed defects concentrated on two different areas. **Figure 7** shows the evolution of the surface defect number 1 through one million loading cycles.

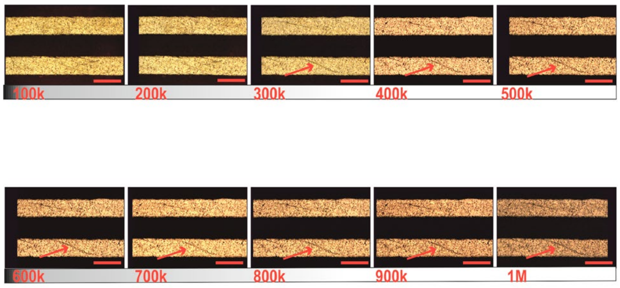

Figure 7 Time series of the defect area 1 through one million cycles. Numbers under the optical images indicate completed loading cycles (i.e., 100k corresponds to 100000 cycles). Red bars indicate 200 µm.

The first surface defect observed after 300k and became more pronounce through time. Surface defect number 2 is shown in **Figure 8.**

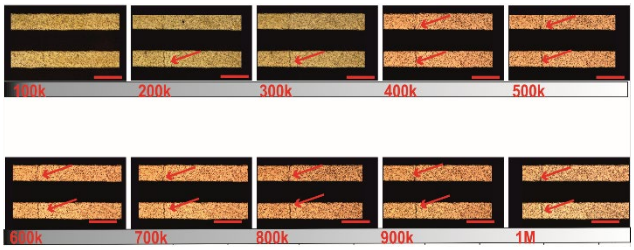

Figure 8 Time series of the defect area 2 through one million cycles. Red bars indicate 200 µm.

The surface defects in defect area 2 were observed after 200k and became more pronounced through time. Both, concentrations and the depth of the defects increased over time. Depth of these surface defects were measured by Zygo white light interference microscopy and measurement result for defect area 1 are shown in **Figure 9**.

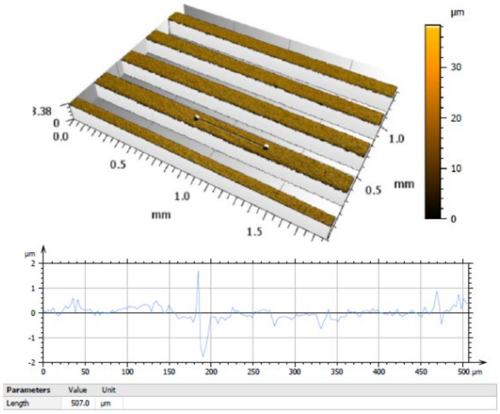

Figure 9 White light interference microscope image of defect area 1 with 5X Michelson objective. The graph shows the surface profile along the line between two spheres.

Depth of these surface defects varies between 1-2 µm according to position of the defect and completed loading cycles. Thickness of the gold combs also measured by Dektak surface profilometer with a stylus that has 12.5 µm radius and measurement resolution of 0.33 µm. Three positions were marked as shown in **Figure 10** and the thickness of the combs were measured along these predefined three lines after each 100k cycles.

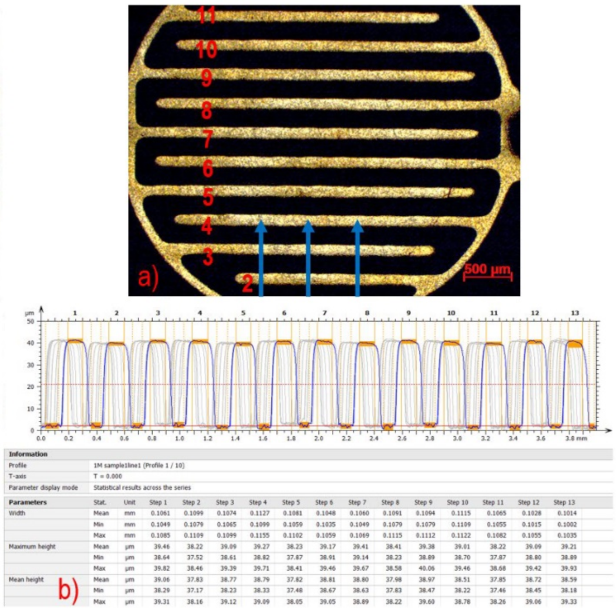

Information	
Profile	1M sample1line1 (Profile 1 / 10)
T-axis	T = 0.000
Parameter display mode	Statistical results across the series

Parameters	Stat.	Unit	Step 1	Step 2	Step 3	Step 4	Step 5	Step 6	Step 7	Step 8	Step 9	Step 10	Step 11	Step 12	Step 13
Width	Mean	mm	0.1061	0.1099	0.1074	0.1127	0.1081	0.1048	0.1060	0.1091	0.1094	0.1115	0.1065	0.1028	0.1014
	Min	mm	0.1049	0.1079	0.1065	0.1099	0.1059	0.1035	0.1049	0.1079	0.1079	0.1109	0.1055	0.1015	0.1002
	Max	mm	0.1085	0.1109	0.1099	0.1155	0.1102	0.1059	0.1069	0.1115	0.1112	0.1122	0.1082	0.1055	0.1035
Maximum height	Mean	µm	39.46	38.22	39.09	39.27	38.23	39.17	39.41	38.41	39.38	39.01	38.22	39.09	39.21
	Min	µm	38.64	37.52	38.61	38.82	37.87	38.91	39.14	38.23	38.89	38.70	37.87	38.80	38.89
	Max	µm	39.82	38.46	39.39	39.71	38.41	39.46	39.67	38.58	40.06	39.46	38.68	39.42	39.93
Mean height	Mean	µm	39.06	37.83	38.77	38.79	37.82	38.81	38.80	37.98	38.97	38.51	37.85	38.72	38.59
	Min	µm	38.29	37.17	38.23	38.33	37.48	38.67	38.63	37.83	38.47	38.22	37.46	38.45	38.18
	Max	µm	39.31	38.16	39.12	39.09	38.05	39.05	38.89	38.22	39.60	38.78	38.26	39.06	39.33

Figure 10 Thickness measurements for gold combs. a) Scanning direction and scanned gold combs are shown as blue arrows and red numbers respectively. b) Thickness deviation from the same direction and on the same combs after one million mechanical load cycles. Gray lines represents the interval measurements (i.e., 200k, 300k, 400k…).

Mean height values were calculated for each comb and each measurement (from 100k to 1M). Corresponding mean thickness for each comb are shown in **Figure 10 b)**. As an example, Step 2 has a mean thickness 37.83 µm. That represents the mean thickness of the gold comb number 2 for 10 measurements. Please note that the difference between min and max values are not more than 1 µm and the resolution of the measurement was 0.33 µm. Data shows no significant thickness change after 1M cycles. Localization of the defects were observed both in simulations (**Figure 1 b**) and in the experimental findings (**Figure 6**).

Surface defects detected on the gold comb structure are not critical to prevent or limit the current flow. In contrast to gold comb, the conductive rubber dome part of the contact can withstand only 300k mechanical load cycles.

5 Discussion

The adhesive friction contact problem was analyzed experimentally. The degradation was identified through microscopic investigation as a fatigue wear problem influenced by adhesive effects between contact surfaces. A sophisticated automatized system was constructed to reproduce such a degradation under controlled conditions of repeated loading cycles. A correlation between simulation and experimental results has been found in terms of localization of the defects. This helps for better understanding the problem and then suggesting a model-based method for an improved design against adhesive wear problem. The simulation tests provide a means to analyze such a contact problem on macro and the micro scale.

As a future perspective, a fatigue model should be implemented in order to realize a predictive capability of wear contact through a computational framework that could be validated on the light of experimental output. Effect of the cycle number and inclination can be implemented to the simulation and theoretical calculations to provide better understanding of the defect mechanism. Although the designed automated system is compact and useful for small scale samples, it can be modified and useful for large scale testing cases (such as wind or snow of the solar panels). In order to achieve more accurate results and mimic the real-life scenarios, local and variable loads can be applied to desired areas.

6 Acknowledgements

Authors would like to thank the Interreg Alpenrhein-Bodensee-Hochrhein for providing the financial support for ABH080 Design Space project and Jerrine Jacob Mathews for supporting design phase of the automated system.

7 Literature

[1] OMRON, Technical Explanation for General-purpose Relays, Accessed on:13.03.21, https://www.ia.omron.com/data_pdf/guide/36/generalrelay_tg_e_10_3.pdf

[2] Koch et al., Dynamic mechanical loading tests on crystalline silicon modules, EU PVSEC Proceedings, 2010, DOI:10.4229/25thEUPVSEC2010-4AV.3.11

[3] R. Mroczkowski, Electronic Connector Handbook: Theory and Applications, McGraw-Hill, London, 1998

[4] ISO 7500-1:2018(en) Calibration and verification of the force-measuring system, 2018

[5] M. Husu. *Wear Prediction for metals*, Tribology International, vol. 30; No. 5, pp. 371-383, 1997

[6] Y. Renard, K. Poulios. GetFEM: Automated FE modeling of multiphysics problems based on a generic weak form language. 2020. Accessed on:13.03.21 https://hal.archives-ouvertes.fr/hal-02532422

[7] Frérot et al., Tamaas: a library for elastic-plastic contact of periodic rough surfaces. Journal of Open Source Sofware, 5, 51, 2020